Title

Cardiotoxicity of environmental contaminant tributyltin involves myocyte oxidative stress and abnormal Ca2+ handling

Authors

Pereira, CLV
Ximenes, CF
Merlo, E
et al.

Publication Date

2019-04-01

DOI

10.1016/j.envpol.2019.01.053

Peer reviewed

HHS Public Access

Author manuscript

Environ Pollut. Author manuscript; available in PMC 2020 December 09.

Published in final edited form as:

Environ Pollut. 2019 April ; 247: 371–382. doi:10.1016/j.envpol.2019.01.053.

Cardiotoxicity of environmental contaminant tributyltin involves myocyte oxidative stress and abnormal Ca^{2+} handling☆

C.L.V. Pereira[a], **C.F. Ximenes**[a], **E. Merlo**[a], **A.S. Sciortino**[a], **J.S. Monteiro**[a], **A. Moreira**[a], **B.B. Jacobsen**[a,c], **J.B. Graceli**[b], **K.S. Ginsburg**[c], **R.F. Ribeiro Junior**[a,c], **D.M. Bers**[c], **I. Stefanon**[a,c,*,1]

[a]Department of Physiology, Federal University of Espírito Santo— UFES, Espírito Santo, Brazil

[b]Department of Morphology, Federal University of Espírito Santo—UFES, Espírito Santo, Brazil

[c]Department of Pharmacology, University of California, Davis, USA

Abstract

Tributyltin (TBT) is an organotin environmental pollutant widely used as an agricultural and wood biocide and in antifouling paints. Countries began restricting TBT use in the 2000s, but their use continues in some agroindustrial processes. We studied the acute effect of TBT on cardiac function by analyzing myocardial contractility and Ca^{2+} handling. Cardiac contractility was evaluated in isolated papillary muscle and whole heart upon TBT exposure. Isolated ventricular myocytes were used to measure calcium (Ca^{2+}) transients, sarcoplasmic reticulum (SR) Ca^{2+} content and SR Ca^{2+} leak (as Ca^{2+} sparks). Reactive oxygen species (ROS), as superoxide anion ($O2^{\bullet-}$) was detected at intracellular and mitochondrial myocardium. TBT depressed cardiac contractility and relaxation in papillary muscle and intact whole heart. TBT increased cytosolic, mitochondrial ROS production and decreased mitochondrial membrane potential. In isolated cardiomyocytes TBT decreased both Ca^{2+} transients and SR Ca^{2+} content and increased diastolic SR Ca^{2+} leak. Decay of twitch and caffeine-induced Ca^{2+} transients were slowed by the presence of TBT. Dantrolene prevented and Tiron limited the reduction in SR Ca^{2+} content and transients. The environmental contaminant TBT causes cardiotoxicity within minutes, and may be considered hazardous to the mammalian heart. TBT acutely induced a negative inotropic effect in isolated papillary muscle and whole heart, increased arrhythmogenic SR Ca^{2+} leak leading to reduced SR Ca^{2+} content and reduced Ca^{2+} transients. TBT-induced myocardial ROS production, may destabilize the SR Ca^{2+} release channel RyR2 and reduce SR Ca^{2+} pump activity as key factors in the TBT-induced negative inotropic and lusitropic effects.

☆This paper has been recommended for acceptance by Dr. Sarah Harmon.

*Corresponding author. Programa de Pós-graduação em Ciências Fisiológicas, Universidade Federal do Espirito Santo, Av Marechal Campos, 1468, Vitoria, ES, Brazil. ivanita@pq.cnpq.br, ivanita.stefanon@ufes.br (I. Stefanon).

[1]Department of Pharmacology, University of California at Davis, 451 Health Sciences Drive, Davis, CA 95616-5270, USA.

Competing financial interests

The authors declare they have no actual or potential competing financial interests.

Keywords

Environmental contaminant; Organotin; Tributyltin; Myocardial contractility; Ca signaling; Sparks; Oxidative stress; Cardiac myocytes; Metal toxicity

1. Introduction

Organotin compounds (OTs), such as tributyltin (TBT), are persistent organometallic environmental contaminants that have been used as components of antifouling paints. TBT has low water solubility and is highly lipophilic. Its high octanol–water partition coefficient (K_{OW}) defined ([TBT] in octanol)/([TBT] in water) is ~10^4 (Bangkedphol et al., 2009). This means that TBT has high bioavailability and is readily absorbed across biological lipid membranes (and may also accumulate in lipophilic compartments such as membranes, lipid droplets and fat). This property gives TBT ready access to intracellular systems, including Ca^{2+}handling processes that we study here. This also means that even low aqueous concentrations (<1 μM) can result in high local membrane concentrations and cytotoxicity.

Although banned by the International Maritime Organization in 2008, TBT is still used in agriculture and other industrial process, especially in some world regions that are not included in the international convention on the control of harmful anti-fouling systems on ships (AFS Convention) or that have limited environmental monitoring (Kotrikla, 2009; Graceli et al., 2013). The main sources of exposure to OTs for humans are through diet, such as ingestion of seafood and contaminated water exposed to antifouling agents or fungicides (Takahashi et al., 1999). Toxicity levels are related to the concentration, time of exposure, bioavailability and sensitivity of the biota, as well as the persistence of OTs in the environment (de Carvalho and Santelli, 2010).

TBT belongs to the obesogens, an endocrine-disrupting chemical (EDC) subclass that can disrupt sensitive metabolic processes if exposure occurs during early development. Obesogens act as metabolic programmers to increase obesity risk (Grun et al., 2006; Janesick and Blumberg, 2011). Several studies have reported important additional toxic TBT effects, including abnormal sex hormone metabolism in rodents (Kishta et al., 2007; Omura et al., 2001), reproductive dysfunctions, irregular estrous cycling, impairment of rat ovary morphophysiology (Delgado Filho et al., 2011; Graceli et al., 2013; Lang et al., 2012), inhibited mitochondrial function (Aldridge et al., 1977), depressed thymus dependent immunity (Miller et al., 1980) and abnormal heme metabolism (Rosenberg et al., 1982).

OTs also affect the cardiovascular system, leading to vascular reactivity abnormalities (dos Santos et al., 2012; Rodrigues et al., 2014; Ronconi et al., 2018) and endothelial dysfunction (Ronconi et al., 2018). We previously demonstrated that even low TBT exposure (100 and 500 ng/kg/bw/day for 15 days) increased reactive oxygen species (ROS) and induced endothelial dysfunction in aorta and mesenteric vessels of female rats (Ribeiro Junior et al., 2016; Rodrigues et al., 2014; Ximenes et al., 2017). OTs appear to inhibit oligomycin-sensitive mitochondrial ATPase/synthase (Mehrotra et al., 1985) the sarcoplasmic reticulum Ca-ATPase (SERCA) (Kodavanti et al., 1991) and plasma membrane Na^+/K^+ ATPase (Cameron et al., 1991). These studies indicate that triorganotin compounds including TBT

may affect the Ca^{2+} handling by altering the function of key cardiac ion transporters, excitation-contraction coupling and mitochondrial function.

Myocardial SERCA is responsible for the re-uptake of cytosolic Ca^{2+} that is required for cardiac relaxation between beats (diastole). During the cardiac action potential, Ca^{2+} enters the cell via the L-type channel and induces further Ca^{2+} release from the sarcoplasmic reticulum (SR) via ryanodine receptors (RyR2). That Ca^{2+}-induced Ca^{2+}-release amplifies the rise in intracellular $[Ca^{2+}]_i$ that activates systolic cardiac contraction (Bers, 2002). Synchronized SR Ca^{2+} release and re-uptake are fundamental for normal systolic and diastolic functioning of cardiomyocytes.

TBT induces reactive oxygen species (ROS) generation and oxidative damage in various systems such as vascular, neural, reproductive, immune, renal, in both *in vivo* and *in vitro* (Ishihara et al., 2012; Katika et al., 2011; Kato et al., 2013; Isomura et al., 2013; Mitra et al., 2015; Nishimura et al., 2015; Rodrigues et al., 2014). ROS can also alter the function of key signaling proteins, e.g. Ca^{2+}/calmodulin-dependent protein kinase II (CaMKII), protein kinase A (PKA), protein kinase C (PKC) and RyR2 (Oda et al., 2015; Wagner et al., 2011). ROS may be harmful when produced in excess due in part to altered ion transport balance (Na^+ and Ca^{2+}) which alters Ca^{2+} handling and promotes both contractile dysfunction and arrhythmias (Kohler et al., 2014).

The present study aims to analyze acute TBT toxicity to myocardial contractility and intracellular Ca^{2+} handling. The hypothesis of this study is that TBT induces cardiotoxicity involving excitation-contraction coupling mechanisms and ROS generation. In order to test this hypothesis we examined the inotropic and lusitropic effects of TBT and its consequence on SR Ca^{2+} leak (assessed as Ca^{2+} sparks), SR Ca^{2+} content in rat ventricular myocytes and the ROS from cytosol and mitochondrial. The myocyte studies support the multicellular data, demonstrating that acute exposure to the environmental contaminant TBT can cause cardiotoxicity. The TBT effects on Ca^{2+} regulatory proteins increase diastolic Ca^{2+} by increasing Ca^{2+} leak, leading to reduced SR Ca^{2+} content and reduced systolic Ca^{2+} transients and contraction.

2. Methods

2.1. Evaluation of the acute effect of TBT on isometric force of papillary muscle

Female Wistar rats (200–250 g) were supplied by the Central Animal Facility of the Federal University of Espírito Santo (Universidade Federal do Espirito Santo, UFES), Espirito Santo, Brazil and were kept in cages with free access to water and food, under temperature control and a light-dark cycle of 12 h. Females were chosen because TBT causes abnormal female sexual development (Grote et al. 2004). All procedures were approved by the UFES Committee for Animal Experiments (CEUA number 27/2016) or NIH Guide for the Care and Use of Laboratory Animals and were approved by Institutional Animal Care and Use Committee at the University of California Davis.

Animals were anesthetized with intraperitoneal injection of ketamine (40 mg/kg, IP) and xylazine (8 mg/kg, IP) and then submitted to thoracotomy. The heart was removed and

retrograde perfused through the aorta with nutrient solution to allow adequate dissection of the anterior and posterior papillary muscles from left ventricle (LV). Papillary muscles were attached to rings and connected to an isometric force transducer (TSD125 - Biopac Systems, Inc.) in a water-jacketed bath, maintained at 30 ± 0.5 °C and containing 20 mL of Krebs-Henseleit solution (KHS): 130 mM NaCl, 1.2 mM $Cacl_2$, 5.4 mM KCl, 2.5 mM $MgSO_4$, 2 mM NaH_2 PO_4, 18 mM $NaHCO_3$, 1.2 mM Na_2SO_4 and 11 mM glucose, gassed with 5% O_2 and 95% CO_2, with pH verified as 7.38 ± 0.02. Field stimulation was provided by isolated rectangular pulses (20 V, 10 ms duration, 0.5 Hz). After gradual fiber stretch to achieve L_{max} (the length at which maximum developed force was attained) and stabilized, isometric force was measured and 1 nM to 10 mM TBT was added to the superfusate, in cumulative fashion, waiting 3 min between increasing concentration and correcting for chamber volume change. TBT was diluted > 100-fold from a stock in 0.4% ethanol.

2.2. Evaluation of cardiac parameters in Langendorff perfused heart system

We used the Langendorff isolated heart perfusion technique to monitor intraventricular pressure during cardiac contraction. The aorta is cannulated and perfused in a retrograde manner to drive coronary artery perfusion throughout the heart. This allows measurement of both coronary perfusion pressure and left ventricular (LV) pressure during constant coronary flow controlled by a peristaltic pump (10 mL/min). Changes in coronary resistance are detect as changes in coronary perfusion pressure (CPP, mmHg) measured by a pressure transducer (TSD 104A-Biopac connected to a Funbec MP-100 preamplifier) connected to the perfusion system. For LV pressure, the left atrium was opened and a water inflatable latex balloon connected to a pressure transducer (Biopac TSD 104A-Biopac connected to a preamplifier) was introduced into the LV. This also allowed control of preload by changing end diastolic pressure (DP, mmHg). Left ventricular isovolumetric systolic pressure (LVISP, mmHg) was measured via a data acquisition system (MP 100, Biopac Systems: Inc; CA, including Biopac Student Lab software), using a sampling rate of 2000 samples/s. Hearts were randomly grouped as Control (perfused with normal KHS) and TBT (exposed 5 min to 50 μM TBT). TBT was diluted in ethanol 0.4% plus 99.6% saline.

2.3. Ventricular function in isolated perfused heart

To analyze heterometric (Frank-Starling) effects, ventricular function curves were obtained by measuring LVISP while the DP was increased from 0 to 30 mmHg in 5 mmHg increments. Frank-Starling relationships were obtained at different perfusate $[Ca^{2+}]$ and upon β-adrenergic stimulation. To evaluate inotropic (homeometric) responses to $[Ca^{2+}]_o$, DP was maintained constant at 10 mmHg and LVISP was recorded during heart perfusion with solutions with $[Ca^{2+}]$ at 0.62; 1.25; 1.87; 2.5 and 3.12 mM. The inotropic response to β-adrenergic activation was analyzed at DP 10 mmHg for a single bolus of 100 μL of 100 μM isoproterenol hydrochloride. Heterometric and homeometric mechanisms were analyzed in the presence and absence of antioxidants: 500 μM Tiron (a superoxide anion ($O_2^{\bullet -}$) scavenger; 100 μM Tempol (4-hydroxy-2,2,6,6-tetramethyl-piperidine-N-oxyl, a superoxide dismutase (SOD) mimetic; 30 μM apocynin (NADPH oxidase inhibitor) and also 10 μM losartan (angiotensin II AT1 receptor blocker).

2.4. Myocardial oxidative stress assay (ROS) by dihydroethidium fluorescence (DHE)

The *in vitro* effects of TBT on myocardial ROS production were measured in the presence of 500 μM Tiron, 100 μM Tempol, 30 μM apocynin and 10 μM losartan. Oxidative fluorescence of dihydroethidium (DHE) was used to evaluate the *in situ* production of $O_2^{\bullet-}$as previously described (Fiorim et al., 2012, Ribeiro et al., 2013). Following the isolated heart procedures, left ventricular (LV) free wall samples approximately 5 mm in length were immersed in Krebs-HEPES buffer solution with 30% sucrose for 1 h, then embedded in cryostat inclusion medium and maintained at −80 °C until cryostat sectioning (10 μm thick), with sections placed on gelatinized slides and frozen. On the analysis day slides were warmed 1 h at 37°C to remove the inclusion medium and then incubated with Krebs-HEPES buffer, for 30 min at 37 °C, dried and incubated with DHE-containing Krebs-HEPES buffer (2 μM) in a chamber protected from light for 30 min. Sections were assembled with mounting medium (Erv-Mount, Easy Path) and coverslip. Heart sections were imaged with an inverted fluorescence microscope (Leica DM 2500) using a 568 nm emission filter at 100 × magnification and photographed with the microscope coupled camera (Leica DFC 310 FX). The mean fluorescence density was calculated using ImageJ.

2.5. Cytosolic, mitochondrial ROS production and mitochondrial membrane potential

Cells were incubated with 5 μM MitoSOX Red (Molecular Probes, Eugene, OR, USA) for 20 min at 37 °C, with 1 μM CM-H_2DCFDA (Molecular Probes, Eugene, OR, USA) for 5 min or 100 nM TMRM (Molecular Probes, Eugene, OR, USA) for 30 min and were subsequently washed with an extracellular solution (Tyrode) that contained 1.2 mM Ca^{2+} to remove the excess of dye. The images were recorded with confocal line-scan imaging using a Zeiss LSM Pascal microscope, with a 40X water-immersive objective. Two-dimensional imaging mode was used, with excitation at 488 and emission at > 517 nm, for CM-H_2DCFDA, alternating with excitation at 532 nm, and emission at > 560 nm for TMRM. Time-lapse x,y images were acquired at 1024 bit resolution and at the sampling rate of 507 ms per frame.

2.6. Cardiomyocyte isolation

Ventricular myocytes were isolated as previously described (Uchinoumi et al., 2016). Briefly, excised hearts were retrograde perfused with collagenase-containing buffer. After myocyte dissociation [Ca^{2+}] was gradually increased from 20 μM to 1 μM over 1 h, in otherwise normal Tyrode's solution (below). Isolated rat ventricular myocytes were transferred to laminin-coated disposable glass coverslips.

2.7. Ca^{2+} transients, SR Ca^{2+} content and Ca^{2+} spark measurements

Intact cardiomyocytes were loaded with 5–10 μM Fluo-4 AM (Molecular Probes, Eugene, OR) for 20–24 min, then perfused with a standard Tyrode's solution containing (in mM) 140 NaCl, 4 KCl, 0–1.2 $CaCl_2$, 1 $MgCl_2$, 5.5 glucose and 10 HEPES, pH 7.4. The indicator was excited at 488 nm (argon laser) with fluorescence measured at >500 nm, using a Biorad Radiance 2100 confocal system. Longitudinal line scans (166 pixels per line) were acquired at 6 ms intervals. Myocytes were electrically stimulated at 0.5 Hz, with just suprathreshold field intensity and pulse duration 2 ms using a pair of platinum electrodes. To determine SR

Ca^{2+} content, electrical stimulation was ceased and the cell was rapidly super-fused with Tyrode's solution with 10 mM caffeine included (after 5 min exposure to TBT at either 10 or 100 nM). Ca^{2+} transients are reported as fluorescence intensity ratio ($\Delta F/F_0$), where F_0 is the resting fluorescence of the cell. The amplitude of caffeine-induced Ca transients was taken as an index of SR Ca^{2+} content. In some experiments 10 μM dantrolene, an inhibitor of Ca^{2+} efflux through RyR, or 10 mM Tiron, a cell permeable superoxide scavenger, was included.

Ca^{2+} spark frequency (CaSpF) was measured in transverse line-scan mode (2 ms/line) before and after exposure to TBT 10 and 100 nM (in sparks.$\mu m^{-1}.s^{-1}$). Spark amplitude, width and duration (as full width or duration at half-maximum) were also measured using the SparkMaster plug-in with ImageJ (Picht et al., 2017) with visual confirmation.

2.8. Permeabilized cardiomyocytes

Cardiomyocytes were suspended in internal solution containing (in mM) 120 K^+-aspartate, 0.5 EGTA, 1.0 $MgCl_2$, 5.0 Na_2-ATP, 10.0 glutathione reductase, 10 creatine phosphokinase, $CaCl_2$ to achieve free Ca^{2+} 10 nM, 5 U/mL creatine phosphokinase, 8% dextran (40,000 Da), 5.0 phosphocreatine di-Na^+ and 10 HEPES (pH 7.2), and placed in the disposable glass chamber for 15 min. The cell membrane was then permeabilized by the addition of saponin 50 μg/mL (quillaja bark purified,-Sigma), with free [Ca^{2+}] buffered at 10 nM. After 30 s, the bath solution was exchanged for an internal solution without saponin and loaded with Fluo-4, 5 K^+ 10 μM, with free [Ca^{2+}] increased to 50 nM Ca^{2+}sparks were recorded with the above mentioned Biorad confocal microscope, using a 40 × oil immersion objective. Fluo-4 was excited at 488 nm and fluorescence was measured at >515 nm. Line scans were made, along the longitudinal axis of the cell, in a central focal plane (scanning speed 166 lines/sec), before and 5 min after TBT exposition. All experiments were performed at room temperature of 25 °C.

2.9. Data analysis

Data are reported as the mean ± SEM values. T-test, One or Two-Way ANOVA test were used to analyze differences between the different groups and followed by Tukey or Bonferroni post-hoc test. $p < 0.05$ was considered significant.

3. Results

3.1. Acute effect of TBT on rat isolated papillary muscle

The effect of increasing TBT concentrations (1 nM–10 mM) on the developed force in papillary muscle is shown in Fig. 1A. There was a gradual negative inotropic response after sequential 3 min exposure to TBT increases up to 100 μM, and a precipitous decline at [TBT] = 1 mM and 10 mM (to 26% and 1% of the initial force, respectively; *$p < 0.05$, n = 6).

3.2. Acute effect of 50 μM TBT on intact isolated hearts

We also measured LV function in Langendorff-perfused hearts upon 5 min exposure to 50 μM TBT at different $[Ca^{2+}]_o$ (0.62–3.12 mM) to test whether TBT inhibited Ca^{2+}-dependent (homeometric) cardiac function. Fig. 1B and E shows that, in the presence of TBT,LVISP

was strongly depressed at normal $[Ca^{2+}]_o$ (1.25 mM: Ctl = 115.1 ± 9.2 vs TBT = 66.6 ± 4* mmHg, n = 7–8, *p < 0.05) and at all higher $[Ca^{2+}]_o$ (1.87, 2.5 and 3.12 mM). Fig. 1C and D shows similar reductions in both maximal LVISP rise (dP/dt+; Ca^{2+} 1.25 mM: Ctl = 3072 ± 184 vs TBT = 1990 ± 227* mmHg/s, n = 7–8, *p < 0.05) and relaxation (dP/dt−; Ca^{2+} 1.87 μM: Ctl = 2530 ± 235 vs TBT = 1792 ± 253* mmHg/s, n = 7–8, *p < 0.05). Fig. 1F demonstrates that DP was also elevated by 50 μM TBT (e.g. at 3.12 mM $[Ca^{2+}]_o$: Ctl = 8.7 ± 0.26 vs TBT = 14.3 ± 3.03 mmHg, n = 6–7,*p < 0.05).

3.3. Myocardial oxidative stress

We examined whether ROS was involved in the negative inotropic effect of TBT at different $[Ca^{2+}]_o$ in hearts perfused with antioxidants: Tiron, Tempol and apocynin and also with the angiotensin II AT1 receptor blocker losartan, a pathway known to induce ROS production. Fig. 2A-D shows that only Tiron, an antioxidant with metal-chelating properties, partially improved the contractility ($[Ca^{2+}]_o$ = 1.25 mM; Ctl = 115 ± 9.3 vs TBT = 66.6 ± 4.1 mmHg *, TBT + Tiron = 86.4 ± 5.1 mmHg$^{\#}$; *p < 0.05 vs Ctl or $^{\#}$TBT). Neither Tempol, apocynin nor losartan had any remedial effect against TBT. Cardiac $O_2^{\bullet-}$ *in situ* production is shown in Fig. 2E. There was a significant increase in $O_2^{\bullet-}$ production in the hearts perfused with TBT, and that was prevented by all of the antioxidants and losartan. These results indicate that the TBT-induced negative inotropy is largely independent of the increased ROS production.

Fig. 3 tests whether TBT (or its induced ROS) influences the Frank-Starling curves as LV preload was increased from 0 to 30 mmHg at low (0.62 mM) and normal $[Ca^{2+}]_o$ (1.25 mM). TBT perfusion (50 μM) significantly reduced LVISP (Fig. 3A and B), but when the curves were normalized (to LVISP at 30 mmHg DP as 100%), the preload-dependence of LVISP was unaltered by TBT (CD). This indicates that the acute TBT effect is not due to a loss of length-dependent activation, such that the heterometric Frank-Starling is preserved.

Perfusion with either antioxidants or AT1 receptor block had no influence on TBT's suppression of contraction at normal $[Ca^{2+}]_o$ (1.25 mM) or high preload (Fig. 3F). However, at lower preloads there was some apparent mitigation of the negative effect of TBT on LVISP (especially for Tiron). At reduced $[Ca^{2+}]_o$ (0.62 mM; Fig. 3E) the negative inotropic effect of TBT was more consistently mitigated by all three antioxidants and losartan. Thus, at low $[Ca^{2+}]_o$, the protective effect of antioxidants and losartan was most evident at low cardiac preload. However, at normal $[Ca^{2+}]_o$ and higher preload levels, ROS suppression may not suffice to protect myocardial contractile strength.

3.4. β-adrenergic response

The β-adrenergic receptor agonist isoproterenol (ISO) was used to test whether acute TBT exposure limited the physiological inotropic and lusitropic responses to ISO, at $[Ca^{2+}]_o$ of 0.62 mM, where baseline contractility was least altered by TBT (Fig. 4). We added a 100 μL bolus of 100 μM ISO to the perfusate and monitored peak functional response during the ensuing 1–5 min. While control hearts showed robust ISO-induced increases in LVISP, it was strongly suppressed by TBT pretreatment (Fig. 4A, D and 4E). The change in LVISP for Control and TBT were 133 ± 9 and 27.1 ± 4.6 mmHg, respectively (Fig. 4A). In addition,

the activation time (AT) and the relaxation time 90% (RT 90%) after ISO were longer in hearts exposed to TBT (Fig. 4B, C, 4E). Neither antioxidants nor losartan prevented the TBT-induced suppression of β-adrenergic-induced inotropic effect (Fig. 4D), although some benefit accrued, again, especially for Tiron.

3.5. Myocyte Ca^{2+} transients, SR Ca^{2+} content and Ca^{2+} sparks

To test whether myocyte Ca^{2+} handling is involved in the negative inotropic effects of TBT, we measured Ca^{2+} transients in isolated ventricular myocytes that were electrically stimulated at 0.5 Hz (Fig. 5). TBT (100 nM) depressed Ca^{2+} transient peaks (Fig. 5A and B), and the rates of twitch $[Ca^{2+}]_i$ decline, indicated by longer time constants (τ) (Ctl = 0.406 ± 0.0445 s, n = 20 vs TBT 100 nM = 0.601 ± 0.057 s n = 17, $p < 0.01$). Higher TBT concentrations tended to cause myocyte death. SR Ca^{2+} content was evaluated by rapid application of 10 mM caffeine to intact ventricular myocytes (Fig. 5C). Cardiomyocytes exposed to 100 nM TBT had significantly reduced SR Ca^{2+} content compared to the control group. The rate of caffeine-induced $[Ca^{2+}]_i$ decline, indicative of Na/Ca exchange dysfunction were also slowed by TBT (τ for Ctl = 3.038 ± 0.385 s, n = 13 vs TBT 100 nM = 4.18 ± 0.34 s, n = 14, $p < 0.03$).

To further test whether there might be enhanced pathological RyR leak (which could cause the observed lower SR Ca^{2+} content), we co-treated isolated cardiomyocytes with 100 nM TBT and 10 μM dantrolene (diastolic RyR channel stabilizer) and the antioxidant Tiron. Fig. 5 shows that both dantrolene and Tiron restored normal SR Ca^{2+} content and twitch Ca^{2+} transient amplitude. Thus, while 100 nM TBT may partially inhibit SERCA2a function (based on twitch $[Ca^{2+}]_i$ decline), the SR Ca leak via RyR is sufficient to explain the reduced SR Ca^{2+} content and twitch Ca^{2+} transients.

We also measured SR Ca^{2+} leak more directly as Ca^{2+} sparks. Ca^{2+} sparks measured in saponin-permeabilized cardiomyocytes are shown in Fig. 6. CaSpF was significantly higher in permeabilized myocytes exposure to 100 nM TBT (Time 5 min: Ctl = 9.7 ± 1.6 vs TBT 16.02 ± 1.3 μm/s). In addition, CaSpF amplitude decreased progressively after 5 min of 100 nM TBT exposure (Ctl = 0.568 ± 0.068 vs TBT 0.342 ± 0.059). This would be consistent with a TBT-induced increase in SR Ca^{2+} leak that reduces SR Ca^{2+} content available for release, explaining smaller twitch Ca^{2+} transients and Ca^{2+} spark amplitude. Dantrolene prevented the TBT-induced Ca^{2+} spark effects on frequency (Ctl = 14.5 ± 0.54 vs TBT 13.6 ± 1.65/sec) and amplitude (Ctl = 0.463 ± 0.017 vs TBT 0.432 ± 0.05). The fractional contribution of SR and NCX/Slow flux were similar in the twitch and caffeine decay in the presence of TBT (data not shown).

3.6. TBT increases cytosolic, mitochondrial ROS production and decreases mitochondrial membrane potential

Since redox homeostasis is determined by the balance between the pro-oxidant and antioxidant, attention must also be given to the mechanisms responsible for intracellular ROS production. We examined cytosolic ROS production by incubating the cells with CM-H_2DCFDA. As shown in Fig. 7A and B, 100 nM TBT increased cytosolic ROS production after 5 min. TBT also decreased mitochondrial membrane potential as shown in Fig. 7C and

D and increased mitochondrial $O2^{\bullet -}$production after 5 min (Fig. 7E and F). Note that the smaller number of cells in the TBT groups reflects in part poorer overall survival of these cells, such that the TBT-induced mitochondrial dysfunction may be underestimated here.

4. Discussion

In this study, we investigated the acute effects of TBT on the heterometric and homeometric mechanisms of cardiac contraction using isolated hearts, papillary muscle and isolated ventricular myocytes from rats. The main result indicates that the acute exposure to TBT is responsible for an intense negative inotropic and lusitropic effect involving impairment SR Ca^{2+} handling.

The heterometric Frank-Starling mechanism is the increase in contractility in response to increasing preload, and it is due both to enhanced myofilament overlap and enhanced myofilament Ca^{2+}sensitivity (ter Keurs, 2012). We analyzed the TBT effects on intact heart length-dependent activation during normalized length-tension curves, by increasing DP and measuring LVISP (Stefanon et al., 1990; Stefanon et al., 1994). TBT induced an acute negative inotropic effect for all DP (Fig. 1B). However, the relative increment on LVISP at both $[Ca^{2+}]_o$ was preserved. We conclude that TBT did not affect the intrinsic Frank-Starling mechanism. While this does not rule out myofilament effects of TBT, we also assessed whether homeometric modulation of cardiac contraction and relaxation were altered (using β-adrenergic activation and altered $[Ca^{2+}]_o$).

The inotropic responses to both increasing $[Ca^{2+}]_o$ and isoproterenol were reduced by TBT compared to the control group in isolated hearts (Figs. 3 and 4). These results suggest that the reduction of contractility might involve alterations of intracellular Ca^{2+}. OTs are known to affect Ca^{2+} transport in diverse cell models (Gennari et al., 2000; Isomura et al., 2013) and also inhibit adenylate cyclase in rat brain, thereby reducing cAMP levels (Leow et al., 1979). Therefore, changes in β-adrenergic responses found in the present study may also be due to decreased cAMP levels or effects on Ca^{2+} handling in the SR. TBT also delayed the kinetics of cardiac muscle contraction (Fig. 4D and E). Three independent variables determine myocardial contractility: the number of active cross-bridges, the rate of the cross-bridge cycle, and the time courses of the onset and offset of cross-bridge interactions. In addition, excitation contraction mechanisms, involving calcium handling, determine the amplitude and kinetics of contraction and relaxation. Thus, changes in the time course of Ca^{2+} delivery and removal can modify the ability of cardiac muscle to do work, and so, control myocardial contractility. It reflects the myocardial fiber shortening and relaxation velocity involving the events of excitation-contraction coupling and contractility mechanisms. Activation time is the time from the onset of contraction to peak tension. It depends on the time to peak of $[Ca^{2+}]_i$, mainly during the phase 2 of action potential and activation kinetics of cross-bridge cycling. The relaxation time is the time from peak tension to the point when tension returns to baseline. During relaxation time, Ca^{2+} is being pumped back into the SR, and the muscle is stretching back to its original length. In the present study, TBT slowed both the activation and relaxation time isoproterenol-activated, demonstrating its cardiotoxicity on the contractility.

Impaired Ca^{2+} reuptake can elevate diastolic $[Ca^{2+}]_i$ and affecting diastolic function and pressure. Indeed, in our study, left ventricle DP increased in the presence of TBT, consistent with this idea.

Kodavanti et al. (1991) found inhibition of cardiac SERCA function by TBT (IC_{50} = 2 μM), and other OTs (triethyltin and trime-thyltin) which would limit Ca^{2+} pumping into the SR, slow relaxation and reduce SR Ca^{2+} content, and could explain the negative inotropic and lusitropic effects of TBT. Consistent with that biochemical data, we found that in intact isolated cardiomyocytes, TBT decreased the amplitude of twitch Ca^{2+} transients, the content of Ca^{2+} in the SR and the apparent rate of SR Ca^{2+} uptake (slower rate of $[Ca^{2+}]_i$ decline). However, TBT also increased CaSpF in permeabilized cardiomyocytes, indicating increased SR Ca leak, which could also explain the TBT-induced reduction of SR Ca^{2+} content (Bers, 2014). We used dantrolene to inhibit Ca^{2+} efflux via RyR, to test whether the TBT-induced increase in SR Ca^{2+} leak was sufficient to explain the reduction in systolic Ca^{2+} transients and the negative inotropic effect of acute TBT exposure in intact hearts. In fact, dantrolene inhibited the TBT-induced SR Ca^{2+} leak and restored normal twitch Ca^{2+} transients (Figs. 5B and 6D). Thus, while TBT inhibited SERCA function by ~50% (based on prolongation in t of $[Ca^{2+}]_i$ decline), the increased SR Ca^{2+} leak may be the major cause of TBT's effect to suppress Ca^{2+} transients and contraction. Such diastolic SR Ca^{2+} leak can also be arrhythmogenic (Bers, 2014) and limit Ca^{2+} transient amplitude (Vassalle and Lin, 2004). We and others have also shown that dantrolene does not inhibit RyR2 in normal physiological conditions, but that dantrolene can restore stable diastolic RyR2 closure during diastole (Oda et al. 2015; Uchinoumi et al. 2016; Maxwell et al., 2012). Indeed, our hypothesis is that TBT is inducing a pathological RyR2 conformation that is partially restored by dantrolene.

The rise in left ventricular DP and diastolic dysfunction during TBT treatment may also be explained by the combination of leaky RyR and reduced SERCA function. In addition, TBT slowed caffeine-induced Ca^{2+} transient decline by the 33%, indicative of a weaker Na/Ca exchange to extrude Ca^{2+} from the myocyte (Bers, 2002). This could be due to either depression of the Na/Ca exchanger function, or elevated $[Na^+]_i$ (secondary to Na/K-ATPase inhibition (Cameron et al., 1991)). In either case, this could also contribute to TBT-induced diastolic dysfunction. A disadvantage of high diastolic Ca^{2+} is the high energy cost to the myocyte and TBT is thought to inhibit mitochondrial ATP production (Matsuno-Yagi and Hatefi, 1993; von Ballmoss et al., 2004).

The mechanism by which TBT acts on RyR2 needs further investigation. RyR2 oxidation can increase SR Ca^{2+} leak and reduce SR Ca^{2+} content, and Ca^{2+} transients (Kohler et al., 2014). Uchinoumi et al. (2016) also showed that H_2O_2-induced RyR2 oxidation reduces the RyR2 calmodulin affinity and leads to a leaky RyR2 conformation. Since TBT promoted ROS production this seems plausible, but ROS scavengers did not prevent the TBT-induced contractile dysfunction or reduced Ca^{2+} transients (Figs. 2 and 5). Thus, TBT might have some other direct or indirect effect to cause SR Ca^{2+} leak.

Other studies have also shown that exposure to TBT increases ROS generation with subsequent oxidative damage in various systems such as vascular, neural, reproductive,

immune, T-lymphocyte cells and neuroblastoma in *in vivo* and *in vitro* models (Katika et al., 2011; Ishihara et al., 2012; Kato et al., 2013; Isomura et al., 2013; Mitra et al., 2015; Nishimura et al., 2015; Rodrigues et al., 2014). Our data are consistent with these findings showing an increase in $O_2^{\bullet-}$ production in hearts perfused with 50 μM TBT as compared to the control group. The increment on $O_2^{\bullet-}$ production was prevented by the antioxidants Tiron, losartan and Tempol. But only Tiron had partial effects to limit contractile dysfunction at $[Ca^{2+}]_o$ above 0.62 mM (Fig. 2). On the other hand, the negative inotropic effect of TBT at low pre-load and low $[Ca^{2+}]_o$ was ameliorated by all antioxidants (Fig. 3). In fact, hearts perfused with either antioxidants or AT1 receptor block, losartan, were not protected against TBT's suppression of contraction at normal $[Ca^{2+}]_o$ (1.25 mM) or high preload. Thus, at low $[Ca^{2+}]_o$, the protective effect of antioxidants and losartan was most evident at low cardiac preload. The present results demonstrated that, at normal $[Ca^{2+}]_o$ and higher preload, ROS suppression may not be enough to protect myocardial contractile against TBT cardiotoxicity. It suggests that TBT might have many different targets in the cardiomyocyte involving its deleterious effect.

These results suggest that the TBT-induced negative inotropy may be at least in part ROS-dependent, especially at low workloads and Ca transients. However, at higher workloads and $[Ca^{2+}]_o$ levels these antioxidants cannot prevent dysfunction. It seems likely that TBT may also have direct effects on the ion transporters discussed, and there is evidence that OTs may interact with SERCA thiol groups resulting in inhibition (Sahib and Desaiah, 1987).

TBT has been identified as a potent inhibitor of mitochondrial ATP synthase (Matsuno-Yagi and Hatefi, 1993, von Ballmoss et al., 200), and that may also participate in the observed contractile dysfunction (both Ca^{2+} handling and contraction rely on ATP). However, the beneficial effects of dantrolene, lead us to conclude that the acute alterations in Ca^{2+} handling and contractile function described here may occur at lower TBT concentration or exposure times than required for profound ATP limitation. But such ATP limitation (suggested by the observed mitochondrial depolarization in Fig. 7D) would certainly further depress cardiac function.

In conclusion, acute exposure to the environmental contaminant TBT causes cardiotoxicity within minutes. We demonstrated that TBT causes negative inotropic and lusitropic effects on the heart, increases ROS and SR Ca^{2+} leak leading to reduced SR Ca^{2+} content. The lower SR Ca^{2+} and slowed reuptake may mediate the negative inotropic and lusitropic effects of TBT.

Acknowledgements

We thank Dr. Christopher Ko for advice during these studies. This research was supported by CAPES; FAPES 03/2017-Universal (179/2017); CNPq (304724/2017-3/12/2017); Edital Universal CNPq (409078/2016-6); EDITAL FAPES 007/2014- Universal Processo 67658016 and US Public Health Service grants (NIH R01-HL030077 and NIH R01-HL092097.

References

Aldridge WN, Street BW, Skilleter DN, 1977 Oxidative phosphorylation. Halide-dependent and halide-independent effects of triorganotin and trioganolead compounds on mitochondrial functions. Biochem. J 15 (3), 353–364, 168.

Bangkedphol S, Keenan HE, Davidson C, Sakultantimetha A, Songsasen A, 2009 The partition behavior of tributyltin and prediction of environmental fate, persistence and toxicity in aquatic environment. Chemosphere 77 (10), 1326–1332. [PubMed: 19846204]

Bers DM, 2002 Cardiac excitation-contraction coupling. Nature 10 (6868), 198–205, 415.

Bers DM, 2014 Cardiac sarcoplasmic reticulum calcium leak: basis and roles in cardiac dysfunction. Annu. Rev. Physiol 76, 107–127. [PubMed: 24245942]

Cameron JA, Kodavanti PR, Pentyala SN, Desaiah D, 1991 Triorganotin inhibition of rat cardiac adenosine triphosphatases and catecholamine binding. J. Appl. Toxicol 11 (6), 403–409. [PubMed: 1662243]

de Carvalho OR, Santelli RE, 2010 Occurrence and chemical speciation analysis of organotin compounds in the environment: a review. Talanta 30 82 (1), 9–24. [PubMed: 20685429]

Delgado Filho VS, Lopes PF, Podratz PL, Graceli JB, 2011 Triorganotin as a compound with potential reproductive toxicity in mammals. Braz. J. Med. Biol. Res 44 (9), 958–965. [PubMed: 21876874]

dos Santos RL, Podratz PL, Sena GC, Filho VS, Lopes PF, Goncalves WL, et al., 2012 Tributyltin impairs the coronary vasodilation induced by 17beta-estradiol in isolated rat heart. J. Toxicol. Environ. Health 75 (16–17), 948–959.

Fiorim J, Ribeiro RF Jr., Azevedo BF, Simoes MR, Padilha AS, Stefanon I, et al., 2012 Activation of K + channels and Na+/K+ ATPase prevents aortic endothelial dysfunction in 7-day lead-treated rats. Toxicol. Appl. Pharmacol 1 (1), 22–31, 262.

Gennari A, Viviani B, Galli CL, Marinovich M, Pieters R, Corsini E, 2000 Organotins induce apoptosis by disturbance of [Ca(2+)](i) and mitochondrial activity, causing oxidative stress and activation of caspases in rat thymocytes. Toxicol. Appl. Pharmacol 1 (2), 185–190, 169.

Graceli JB, Sena GC, Lopes PF, Zamprogno GC, da Costa MB, Godoi AF, et al., 2013 Organotins: a review of their reproductive toxicity, biochemistry, and environmental fate. Reprod. Toxicol 36, 40–52. [PubMed: 23228341]

Grote K, Stahlschmidt B, Talsness CE, Gericke C, Appel KE, Chahoud I, 2004 Effects of organotin compounds on pubertal male rats. Toxicology 1 (3), 145–158, 202.

Grun F, Watanabe H, Zamanian Z, Maeda L, Arima K, Cubacha R, et al., 2006 Endocrine-disrupting organotin compounds are potent inducers of adipogenesis in vertebrates. Mol. Endocrinol 20 (9), 2141–2155. [PubMed: 16613991]

Ishihara Y, Kawami T, Ishida A, Yamazaki T, 2012 Tributyltin induces oxidative stress and neuronal injury by inhibiting glutathione S-transferase in rat organotypic hippocampal slice cultures. Neurochem. Int 60 (8), 782–790. [PubMed: 22449404]

Isomura M, Kotake Y, Masuda K, Miyara M, Okuda K, Samizo S, et al., 2013 Tributyltin-induced endoplasmic reticulum stress and its Ca(2+)-mediated mechanism. Toxicol. Appl. Pharmacol 1 (1), 137–146, 272.

Janesick A, Blumberg B, 2011 Endocrine disrupting chemicals and the developmental programming of adipogenesis and obesity. Birth Defects Res C Embryo Today 93 (1), 34–50. [PubMed: 21425440]

Katika MR, Hendriksen PJ, van LH, Peijnenburg A, 2011 Exposure of Jurkat cells to bis (tri-n-butyltin) oxide (TBTO) induces transcriptomics changes indicative for ER-and oxidative stress, T cell activation and apoptosis. Toxicol. Appl. Pharmacol 1 254 (3), 311–322. [PubMed: 21601586]

Kato T, Tada-Oikawa S, Wang L, Murata M, Kuribayashi K, 2013 Endocrine disruptors found in food contaminants enhance allergic sensitization through an oxidative stress that promotes the development of allergic airway inflammation. Toxicol. Appl. Pharmacol 15 (1), 10–18, 273.

Kishta O, Adeeko A, Li D, Luu T, Brawer JR, Morales C, et al., 2007 In utero exposure to tributyltin chloride differentially alters male and female fetal gonad morphology and gene expression profiles in the Sprague-Dawley rat. Reprod. Toxicol 23 (1), 1–11. [PubMed: 17095186]

Kodavanti PR, Cameron JA, Yallapragada PR, Vig PJ, Desaiah D, 1991 Inhibition of Ca2+ transport associated with cAMP-dependent protein phosphorylation in rat cardiac sarcoplasmic reticulum by triorganotins. Arch. Toxicol 65 (4), 311–317. [PubMed: 1659351]

Kohler AC, Sag CM, Maier LS, 2014 Reactive oxygen species and excitation-contraction coupling in the context of cardiac pathology. J. Mol. Cell. Cardiol 73, 92–102. [PubMed: 24631768]

Kotrikla A, 2009 Environmental management aspects for TBT antifouling wastes from the shipyards. J. Environ. Manag 90 (Suppl. 1), S77–S85.

Lang PP, Delgado Filho VS, Lopes PF, Cavati SG, Matsumoto ST, Samoto VY, et al., 2012 Tributyltin impairs the reproductive cycle in female rats. J. Toxicol. Environ. Health 75 (16–17), 1035–1046.

Leow AC, Towns KM, Leaver DD, 1979 Effect of organotin compounds and hexachlorophene on brain adenosine cyclic 3',5'-monophosphate metabolism. Chem. Biol. Interact 27 (1), 125–132. [PubMed: 225045]

Matsuno-Yagi A, Hatefi Y, 1993 Studies on the mechanism of oxidative phosphorylation. ATP synthesis by submitochondrial particles inhibited at F0 by venturicidin and organotin compounds. J. Biol. Chem 25 (9), 6168–6173, 268.

Maxwell JT, Domeier TL, Blatter LA, 2012 Dantrolene prevents arrhythmogenic Ca2+ release in heart failure. Am. J. Physiol. Heart Circ. Physiol 15 302 (4), H953–H963. [PubMed: 22180651]

Mehrotra BD, Prasada Rao KS, Desaiah D, 1985 Effect of plictran on beef heart mitochondrial ATPases. Toxicol. Lett 26 (1), 25–30. [PubMed: 3161218]

Miller RR, Hartung R, Cornish HH, 1980 Effects of diethyltindichloride on amino acid and nucleoside transport in suspended rat thymocytes. Toxicol. Appl. Pharmacol 30 (3), 564–571, 55.

Mitra S, Siddiqui WA, Khandelwal S, 2015 Differential susceptibility of brain regions to tributyltin chloride toxicity. Environ. Toxicol 30 (12), 1393–1405. [PubMed: 24895210]

Nishimura T, Duereh M, Sugita Y, Yoshida Y, Higuchi K, Tomi M, et al., 2015 Protective effect of hypotaurine against oxidative stress-induced cytotoxicity in rat placental trophoblasts. Placenta 36 (6), 693–698. [PubMed: 25801460]

Oda T, Yang Y, Uchinoumi H, Thomas DD, Chen-Izu Y, Kato T, et al., 2015 Oxidation of ryanodine receptor (RyR) and calmodulin enhance Ca release and pathologically alter, RyR structure and calmodulin affinity. J. Mol. Cell. Cardiol 85, 240–248. [PubMed: 26092277]

Omura M, Ogata R, Kubo K, Shimasaki Y, Aou S, Oshima Y, et al., 2001 Two-generation reproductive toxicity study of tributyltin chloride in male rats. Toxicol. Sci 64 (2), 224–232. [PubMed: 11719705]

Picht E, Zima AV, Blatter LA, Bers DM, 2017 SparkMaster: automated calcium spark analysis with ImageJ. Am. J. Physiol. Cell Physiol 293 (3), C1073–C1081.

Ribeiro RF Jr., Potratz FF, Pavan BM, Forechi L, Lima FL, Fiorim J, et al., 2013 Carvedilol prevents ovariectomy-induced myocardial contractile dysfunction in female rat. PLoS One 8 (1) e53226. [PubMed: 23308166]

Ribeiro RF Junior, Marques VB, Nunes DO, Ronconi KS, Araujo JF, Rodrigues PL, et al., 2016 Tributyltin chloride increases phenylephrine-induced contraction and vascular stiffness in mesenteric resistance arteries from female rats. Toxicol. Appl. Pharmacol 15 (295), 26–36.

Rodrigues SM, Ximenes CF, de Batista PR, Simoes FV, Coser PH, Sena GC, et al., 2014 Tributyltin contributes in reducing the vascular reactivity to phenylephrine in isolated aortic rings from female rats. Toxicol. Lett 21 (3), 378–385, 225.

Ronconi KS, Stefanon I, Ribeiro RF Junior, 2018 Tributyltin and vascular dysfunction: the role of oxidative stress. Front. Endocrinol 12 (9), 354.

Rosenberg DW, Drummond GS, Kappas A, 1982 The influence of organometals on heme metabolism. In vivo and in vitro studies with organotins. Mol. Pharmacol 21 (1), 150–158. [PubMed: 6897100]

Sahib IK, Desaiah D, 1987 Inhibition of beta-adrenergic stimulated calcium pump of rat cardiac sarcoplasmic reticulum by tricyclohexyltin hydroxide. Cell Biochem. Funct 5 (2), 149–154. [PubMed: 2953502]

Stefanon I, Vassallo DV, Mill JG, 1990 Left ventricular length dependent activation in the isovolumetric rat heart. Cardiovasc. Res 24 (3), 254–256. [PubMed: 2346960]

Stefanon I, Auxiliadora-Martins M, Vassallo DV, Mill JG, 1994 Analysis of right and left ventricular performance of the rat heart with chronic myocardial infarction. Braz. J. Med. Biol. Res 27 (11), 2667–2679. [PubMed: 7549991]

Takahashi S, Mukai H, Tanabe S, Sakayama K, Miyazaki T, Masuno H, 1999 Butyltin residues in livers of humans and wild terrestrial mammals and in plastic products. Environ. Pollut 106 (2), 213–218. [PubMed: 15093048]

ter Keurs HE, 2012 The interaction of Ca2+ with sarcomeric proteins: role in function and dysfunction of the heart. Am. J. Physiol. Heart Circ. Physiol 1 302 (1), H38–H50. [PubMed: 22021327]

Uchinoumi H, Yang Y, Oda T, Li N, Alsina KM, Puglisi JL, et al., 2016 CaMKII-dependent phosphorylation of RyR2 promotes targetable pathological RyR2 conformational shift. J. Mol. Cell. Cardiol 98, 62–72. [PubMed: 27318036]

Vassalle M, Lin CI, 2004 Calcium overload and cardiac function. J. Biomed. Sci 11 (5), 542–565. [PubMed: 15316129]

von Ballmoss C, Brunner J, Dimroth P, 2004 The ion channel of F-ATP synthase is the target of toxic organotin compounds. Proc. Natl. Acad. Sci. U S A 3 101 (31), 11239–11244. [PubMed: 15277681]

Wagner S, Ruff HM, Weber SL, Bellmann S, Sowa T, Schulte T, et al., 2011 Reactive oxygen species-activated Ca/calmodulin kinase IIdelta is required for late I(Na) augmentation leading to cellular Na and Ca overload. Circ. Res 4 108 (5), 555–565. [PubMed: 21252154]

Ximenes CF, Rodrigues SML, Podratz PL, Merlo E, de Araujo JFP, Rodrigues LCM, et al., 2017 Tributyltin chloride disrupts aortic vascular reactivity and increases reactive oxygen species production in female rats. Environ. Sci. Pollut. Res. Int 24 (31), 24509–24520. [PubMed: 28900851]

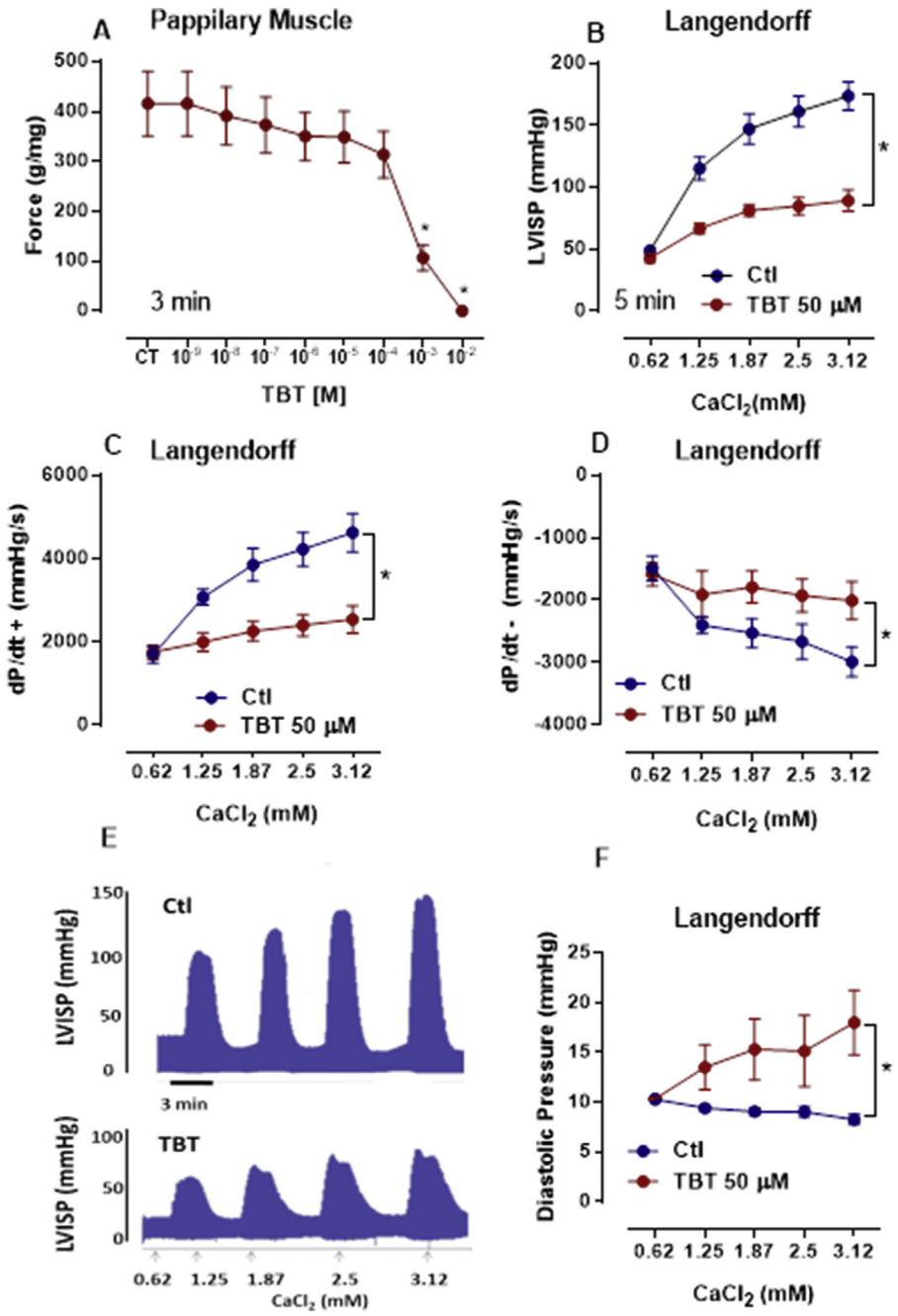

Fig. 1.

Isolated papillary muscle: A) Inotropic response to TBT (1 nM–10 mM; 3 min exposure) on developed force (g/mg) (n = 6). Langendorff perfused heart: B) Change in the left ventricle isovolumic systolic pressure (LVISP, mmHg), C) First positive derivative of pressure (dP/dt +, mmHg/s), D) First negative derivative of pressure (dP/dt−, mmHg/s) during increments of extracellular Ca^{2+} from 0.62 to 3.12mM in the Langendorff perfused hearts, Control group (Ctl, n = 7 rats),TBT (50 µM, n = 8). E) Representative record of LVISP during increment of extracellular Ca^{2+} from 0.62 to 3.12 mM for Ctl and TBT groups during increment of extracellular Ca^{2+} from 0.62 to 3.12 mM. F) Diastolic pressure (DP, mmHg) during

increment of Ca^{2+} in the Ctl and TBT group (TBT 50 μM, n = 8 rats). Results are reported as mean ± SEM. *p < 0.05 TBT vs Ctl, two-way ANOVA plus Tukey post hoc.

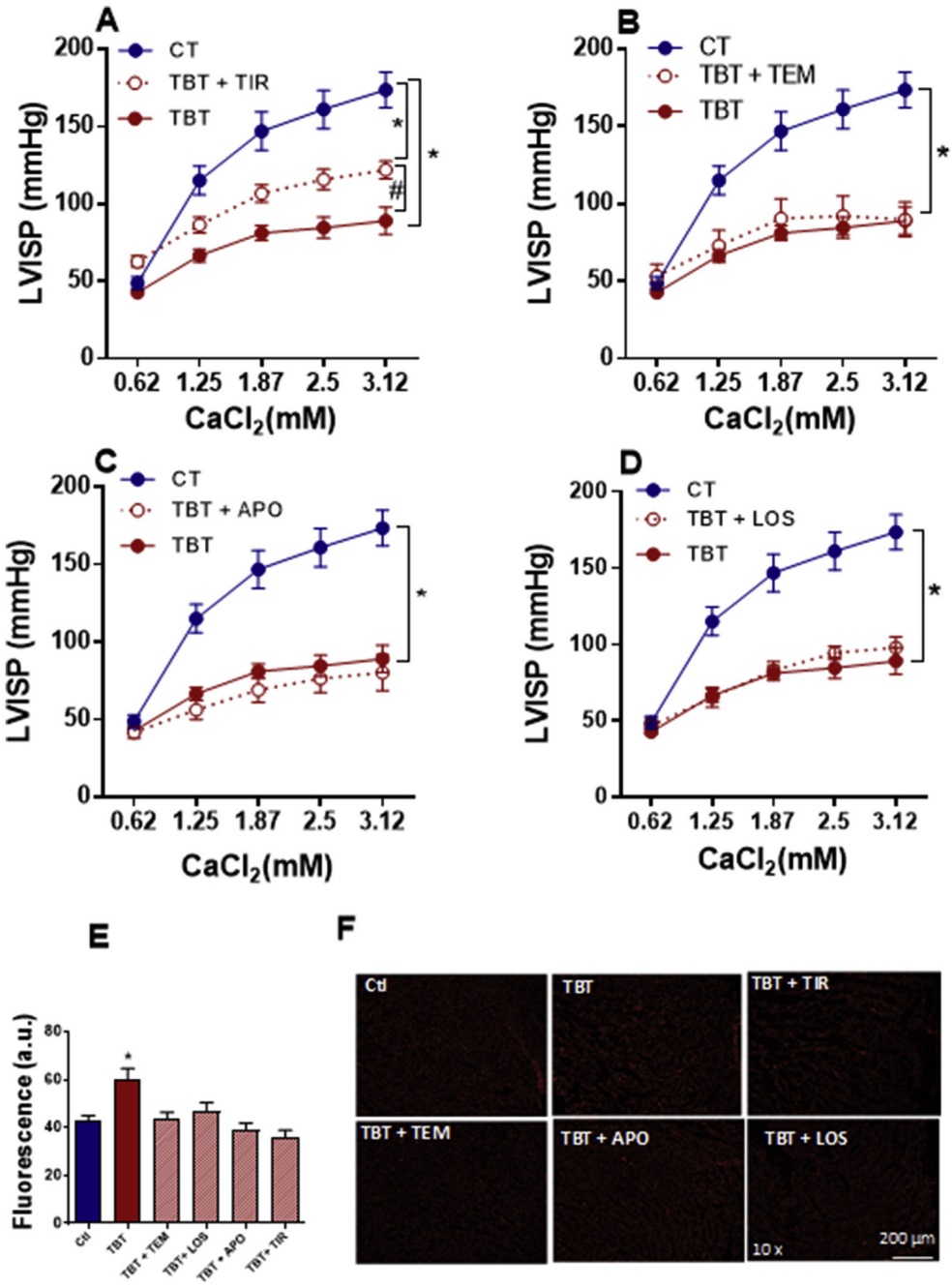

Fig. 2.

Effects of antioxidants during increment of extracellular Ca^{2+} from 0.62 to 3.12 mM in the Langendorff perfused hearts. A) Groups Ctl, TBT (50 μM) and TBT + Tiron (500 μM); B) Groups Ctl, TBT and TBT + Tempol (100 μM); C) Groups Ctl, TBT and TBT + Apocynin (30 μM) and D) Ctl, TBT and TBT + Losartan (10 μM). E) *In vitro* detection of superoxide anion ($O2^{\bullet -}$) after TBT (50 μM) incubation in the presence and absence of antioxidants. Heart fluorescence micrographs were stained with DHE (red fluorescence) sensitive dye for the Ctl (n = 4 rats), TBT (n = 4 rats), TBT + Tiron (500 μM) (n = 4 rats) groups, TBT +

Tempol (100 μM) (n = 4 rats) and TBT + Losartan (10 μM) (n = 4 rats). Results are reported as mean ± SEM. *p < 0.05 vs Ctl, #p < 0.05 vs TBT, two way ANOVA plus Tukey post hoc.

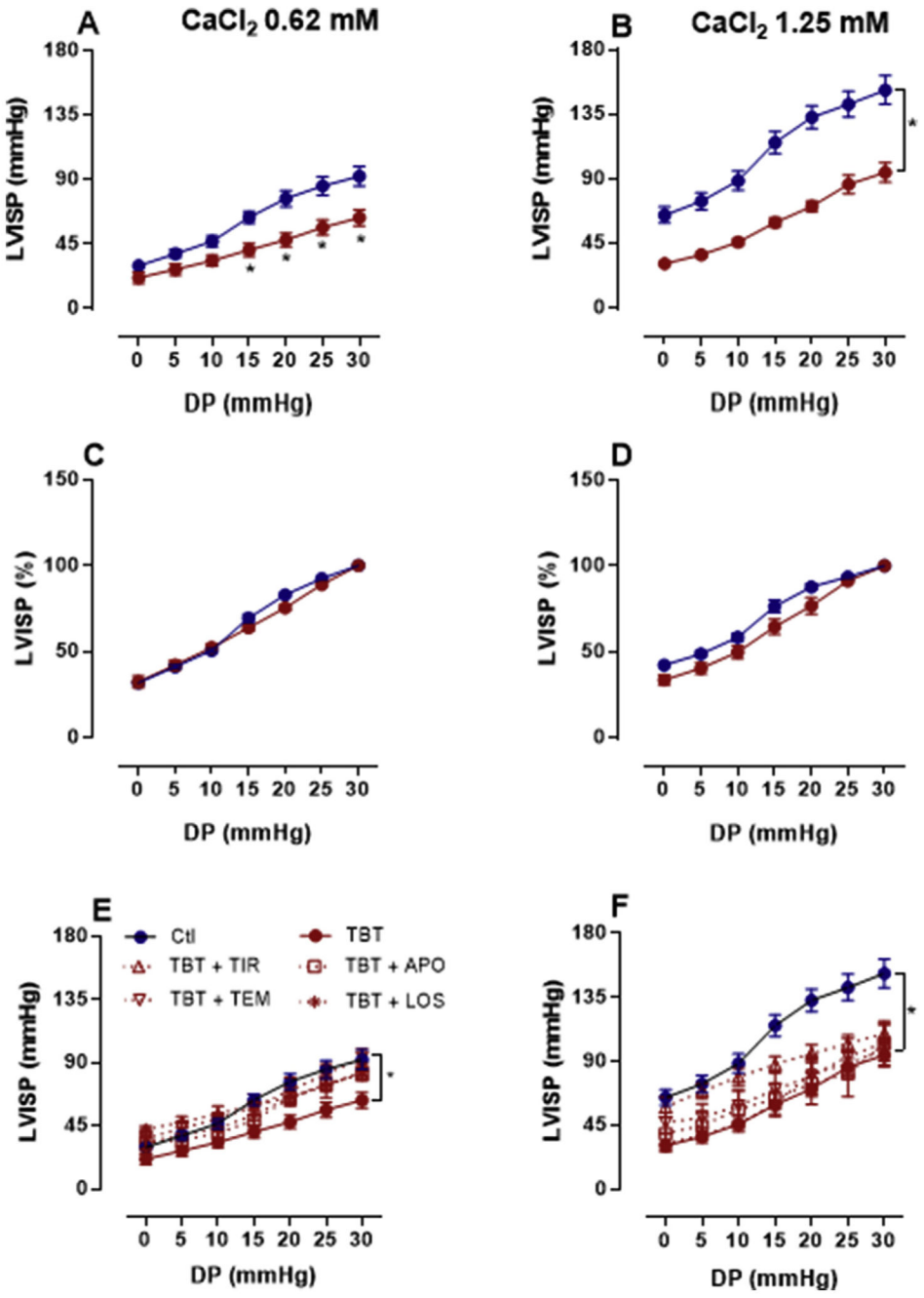

Fig. 3.

Left ventricular isovolumetric systolic pressure (LVISP, mmHg) and diastolic pressure (DP, mmHg) in 0,62 mM Ca^{2+} (A, C, E) and 1,25 mM Ca^{2+} (B, D, F). A and B represent absolute increment on LVISP (mmHg). C and D represent % increment in the LVISP considering its value at 30 mmHg DP as 100%. E and F show the increment on LVISP in the groups control (Ctl), TBT (50 μM) and TBT + Tiron (500 μM); B: Groups Ctl, TBT and TBT + Tempol (100 μM); C: Groups Ctl, TBT and TBT + Apocynin (30 μM) and D: Ctl, TBT and TBT + Losartan groups (10 μM). Results are reported as mean ± SEM. *p < 0.05 TBT vs Ctl, #p < 0.05 TBT + Tempol vs TBT, two way ANOVA; n = 7–8 per group.

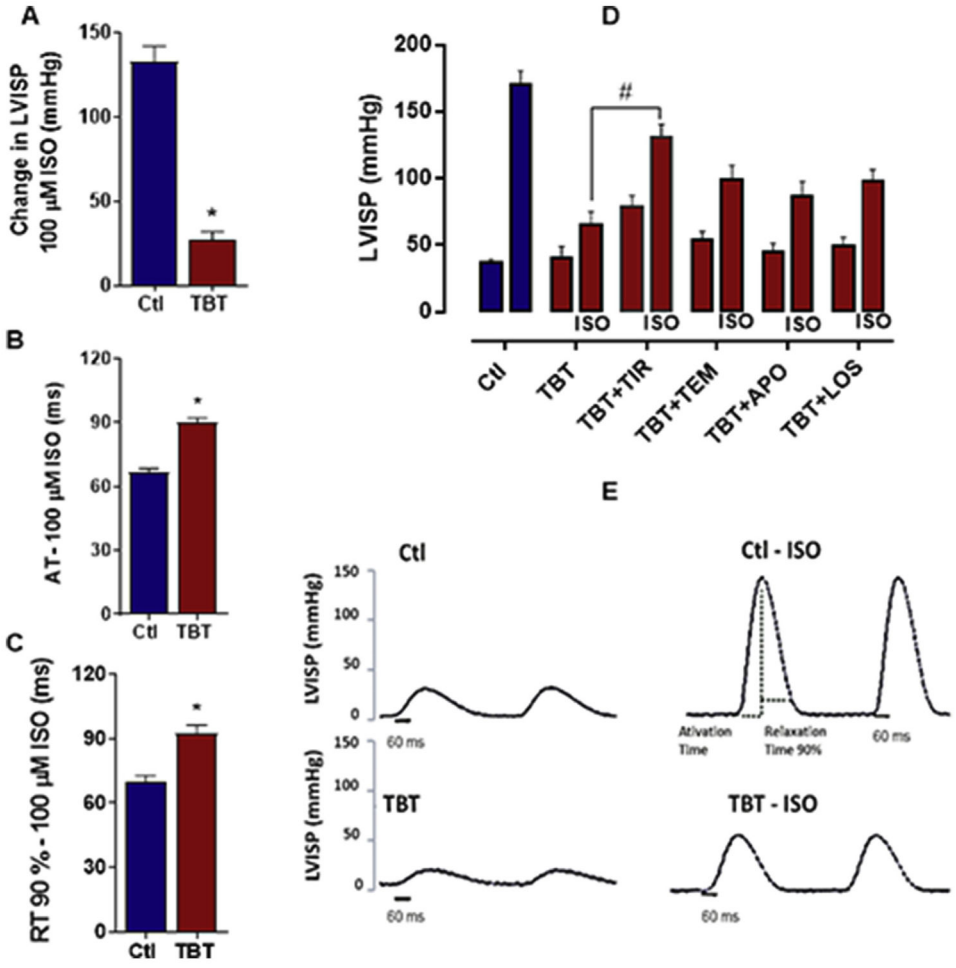

Fig. 4.

Effect of 100 µM Isoproterenol (ISO) in the Langendorff isolated perfused heart: A) Change in the left ventricular isovolumetric systolic pressure (LVISP, mmHg) before and after ISO; B) AT: Activation Time (ms); C) RT: Relaxation Time 90% (ms); D) LVISP in the control group (Ctl) and TBT perfusion, before and after ISO, in the presence and absence of antioxidants: Tiron, Tempol, Apocynin and angiotensin II blocker, Losartan; E) Representative record of LVISP in the Ctl and TBT 50 µM before and after 100 µM ISO, showing also the way activation and relaxation time (AT and RT) were measured (*$p < 0.05$ vs Ctl; #$p < 0.05$ TBT + ISO vs TBT + ISO + Tiron); n = 7–8 per group.

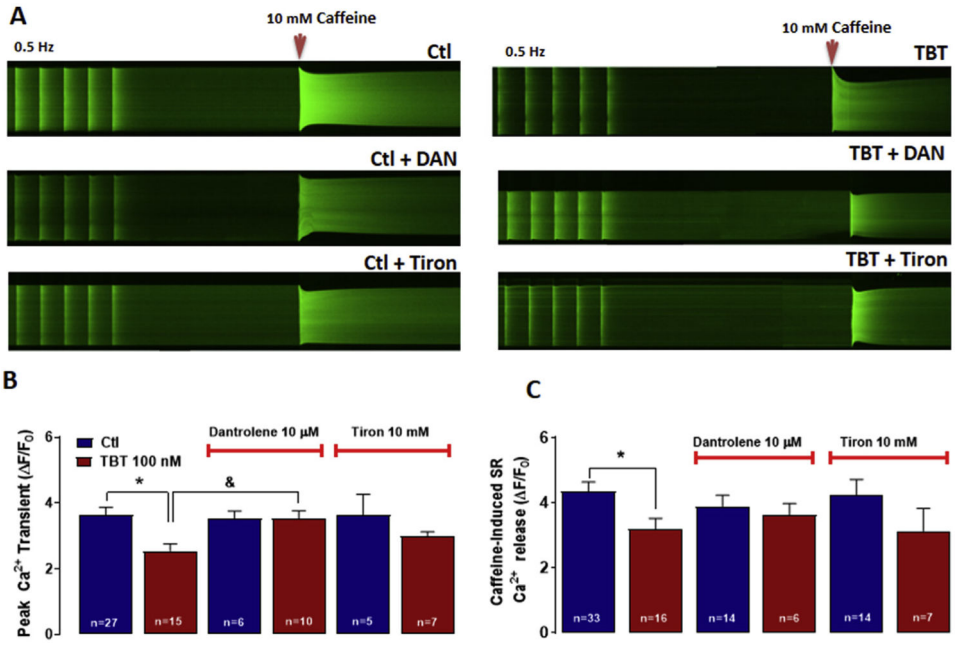

Fig. 5.

Ca^{2+} transient (CaT) amplitude during 0.5 Hz pacing and SR Ca^{2+} content (10mM Caffeine) in rat intact cardiomyocytes of Control (Ctl), TBT groups in the presence and absence of dantrolene 10 µM (DAN) and 10 mM Tiron. A) Representative confocal images of caffeine-induced CaT and SR Ca^{2+} content in the absence (Ctl, Ctl + DAN and Ctl + Tiron) and presence of 100 nM (TBT, TBT + DAN and TBT + Tiron). B) Peak of Ca^{2+} Transient ($\Delta F/F_0$) and C) Caffeine-iInduced SR Ca^{2+} release ($\Delta F/F_0$). Dantrolene and Tiron suppressed the TBT effect on Ca^{2+} transient and caffeine-induced SR Ca^{2+} release. The fluorescence data were normalized as $\Delta F/F_0$. Results are reported as mean ± SEM. *$p < 0.05$ TBT vs Ctl; &TBT vs TBT + DAN, n = number of cells.

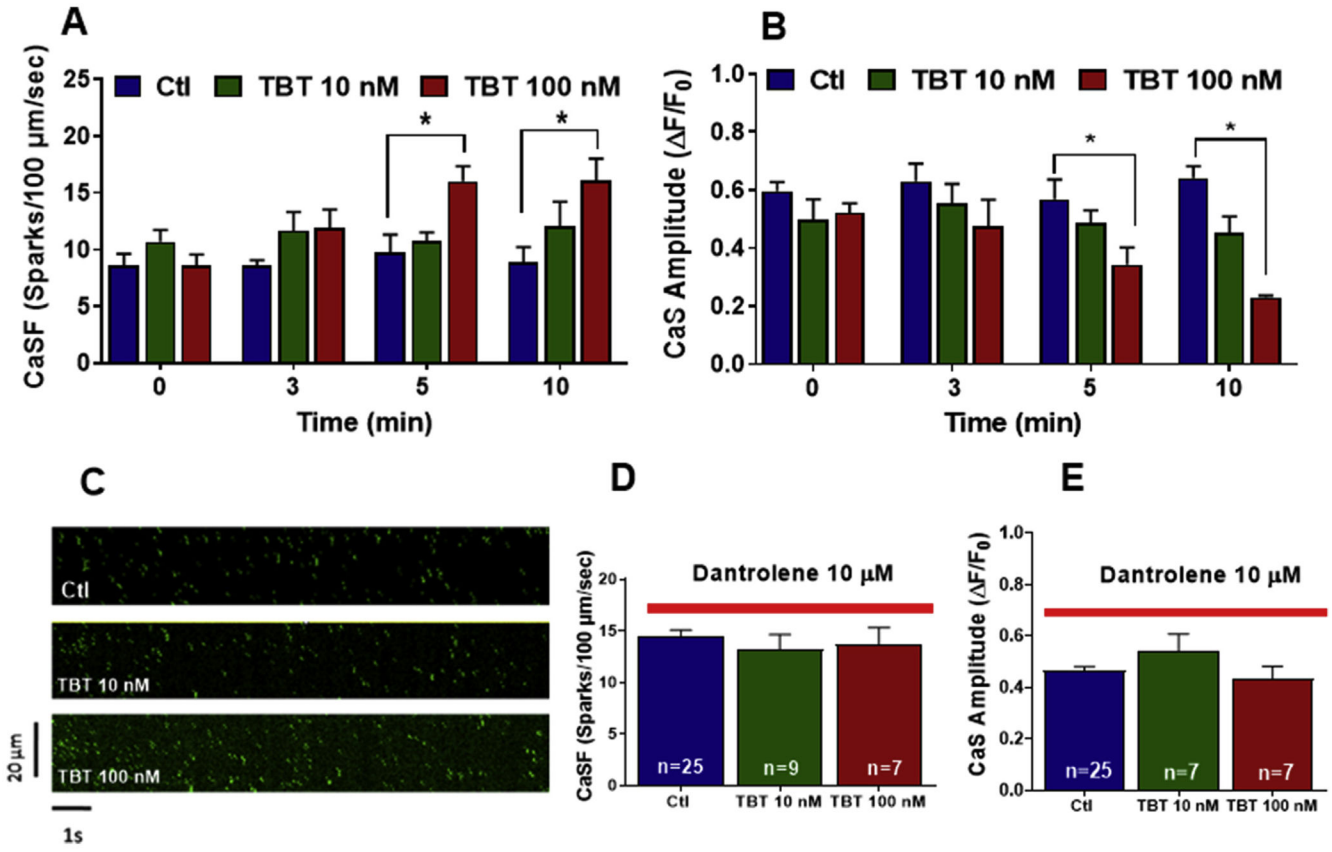

Fig. 6.

Ca^{2+} Sparks analysis in rat permeabilized cardiomyocytes at 0, 3, 5 and 10 min in control condition (Ctl) and in the presence of 10 nM and 100nM TBT: A) Calcium Sparks Frequency (CaSF, Sparks/100 µm/s) and B) Calcium Sparks Amplitude (CaS Amplitude, $\Delta F/F_0$), n = 5–6 cells per group; C) Representative records of calcium sparks 10 min after, control condition (Ctl), 10 nM and 100 nM TBT; D) Calcium Sparks Amplitude and E) Calcium Sparks Frequency in the presence of 10 µM Dantrolene after 5 min TBT exposition. Results are reported as mean ± SEM. *$p < 0.05$ vs Ctl, two way ANOVA, n = number of cells.

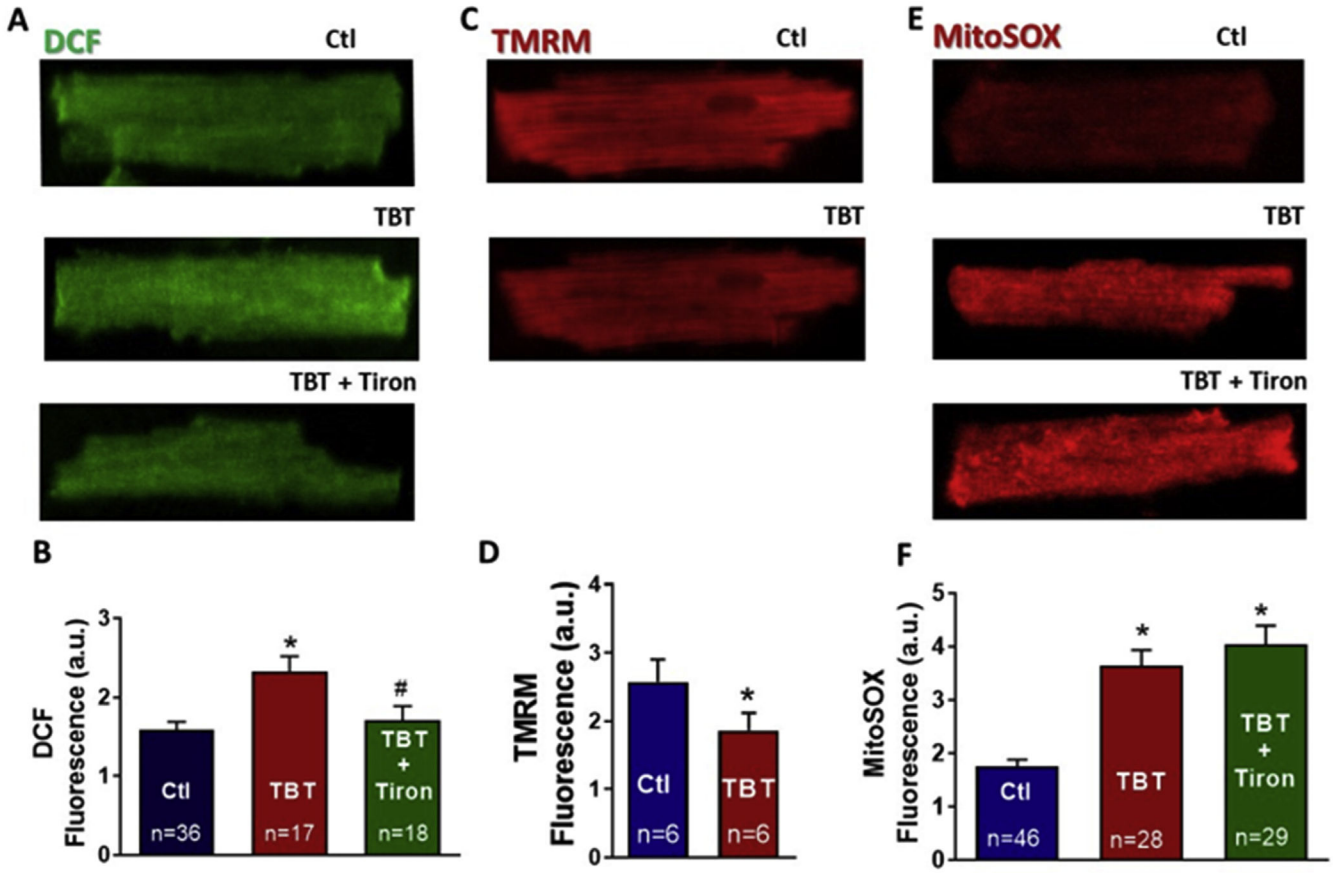

Fig. 7.

Cytosolic (DCF), mitochondrial (MitoSOX) ROS production and mitochondrial membrane potential (TMRM) in the control Ctl and TBT groups treated or not with 10 mM Tiron. Cells were incubated for 5 min with: A and B) 1 μM DCF; C and D) 100 nM TMRM and E and F) 5 μM MitoSOX Red, The images were recorded with confocal line-scan imaging using a Zeiss LSM Pascal microscope, with a 40X water-immersive objective. *$p < 0.05$ vs Ctl.; #$p < 0.05$ vsTBT, n = number of cells.